Comparative analysis of flood and rainfall frequency in the ungauged sub-watersheds of Kakia and Esamburumbur in Narok town, Kenya, using the EBA4SUB rainfall-runoff model

Eva Audrey Yessito Houessou-Dossou,[1] John Mwangi Gathenya,[2] Mugwima Njuguna,[3] Zachary Abiero Gariy,[4] Andrea Petroselli[5]

[1]Civil Engineering Department, Pan African University-Institute for Basics Sciences, Technology and Innovation/ Jomo Kenyatta University of Agriculture and Technology, Nairobi, Kenya; [2]Soil, Water and Environmental Engineering Department/Jomo Kenyatta University of Agriculture & Technology, Nairobi, Kenya; [3]Centre for Urban Studies, School of Architecture & Building Sciences/Jomo Kenyatta University of Agriculture & Technology, Nairobi, Kenya; [4]School of Civil, Environmental & Geospatial Engineering/Jomo Kenyatta University of Agriculture & Technology, Nairobi, Kenya; [5]Department of Economics, Engineering, Society and Business, Tuscia University, Viterbo, Italy

Correspondence: Eva Audrey Yessito Houessou-Dossou, Civil Engineering Department, Pan African University-Institute for Basics Sciences, Technology and Innovation/Jomo Kenyatta University of Agriculture and Technology, P.O. Box 62000-00200 Nairobi, Kenya.
Tel.: +254.743607745 / +229.66434697.
E-mail: houessoudossoueva@yahoo.com

Key words: Design hydrograph; EBA4SUB; flood frequency; rainfall frequency; return period.

Acknowledgements: the authors are grateful to the Pan African University-Institute for Basic Sciences Technology and Innovation, Kenya.

Funding: this study was partly supported by funds from the project - *Flash floods and erosion in Enkare Narok Basin: Causes and Management* - funded by the National Research Fund of Kenya under the Multi-disciplinary Research Grants 2016/2017. We acknowledge support from partners, the Water Resources Authority and Ewaso Ngiro South Development Authority.

Conflict of interest: the authors declare no conflict of interest.

Received for publication: 10 November 2021.
Accepted for publication: 1 February 2022.

Journal of Agricultural Engineering 2022; LIII:1307
doi:10.4081/jae.2022.1307

Abstract

Knowledge of design peak flow is crucial in various hydrology, hydraulics, and water resources management applications. However, obtaining design peak flow is challenging, especially in ungauged basins lacking discharge observations, a circumstance that does not allow the calibration of advanced hydrological models. Recently, a new method called EBA4SUB (event-based approach for small and ungauged basins) was introduced to estimate the design peak flow and hydrograph in ungauged basins. The current study used the EBA4SUB model to evaluate the design peak flow in the Kakia and Esamburumbur sub-watersheds, Narok town, Kenya. The study investigated the link between rainfall frequency analysis and flood frequency analysis, showing the reliability of this approach to model at event scale the selected watersheds. Furthermore, the coefficient of determination between the rainfall-based return period and the flow-based return period in both the Kakia and Esamburumbur sub-watersheds highlighted the strong dependency between design rainfall and design peak flow.

Introduction

Design peak flow estimation is crucial in many environmental studies and hydraulic applications, from floods and droughts modelling to the construction of hydraulic structures. However, design peak flow estimations are tricky, particularly in ungauged watersheds (Jian *et al.,* 2017). This challenge is of the utmost importance in Africa due to the lack of long-term hydrological records in many local watersheds (Ahmed *et al.,* 2019). Many solutions have been put in place by researchers to address this issue. One of these is the regionalisation approach that is used to switch peak flow information from a gauged watershed (donor) to an ungauged (target) watershed (Yang *et al*., 2018). This approach has shown outstanding results in different parts of the world (Beck *et al*., 2016; Pagliero *et al*., 2019; Song *et al.,* 2016; Virães and Cirilo, 2019). While the regionalisation method has proved its reliability, long-term discharge data are still needed from the donor watershed. However, the correct donor with these characteristics cannot be easily identified. A different method for estimating the design peak flow is by using conceptual formulas, like the well-known rational formula, which was primarily developed for small watersheds (Dhakal *et al*., 2012). Due to its simplicity and the minimal need for input data, the rational formula is commonly used.

Nonetheless, the implementation of this method raises some drawbacks. Grimaldi and Petroselli (2015) emphasised some of them, mainly the uncertainty in the determination of the runoff coefficient and the assumption of the critical rainfall duration that may lead to an underestimation of the peak flow. Grimaldi and Petroselli (2015) and Piscopia *et al*. (2015), therefore, introduced a new approach called event-based approach for small and ungauged basins (EBA4SUB), which aims at minimising the user subjectivity to determine flow hydrograph in ungauged watersheds, using the same information needed for the rational formula. EBA4SUB is based on the watershed topography thanks to the digital elevation model (DEM) and uses the intensity-duration-frequency (IDF) curves for assessing the design rainfall. Moreover, for excess rainfall estimation and runoff propagation, it is able to automatically estimate the model parameters, although the user can modify the suggested values if more information is available. So far, the method has shown promising results. Recanatesi *et al*. (2017) and Recanatesi and Petroselli (2020) applied the model for flood mapping in a suburban watershed of the metropolitan area of Rome, Italy. Petroselli and Grimaldi (2018) evaluated the performance of the model for design flow estimation over four watersheds in Europe (Italy, France, and Germany). Młyński *et al*. (2018, 2020a,b) applied the model for determining the design hydrograph in selected mountainous catchments of southern Poland. Nardi, Annis and Biscarini (2018) used the model to investigate the causes of the increase in urban floods in the small watershed area of Rome. Petroselli *et al*. (2019a,b,c) performed applications in various small watersheds located in different countries (Iran, Bosnia and Herzegovina, Slovakia) and with different geomorphologic characteristics as well as different climatic regimes. Recently, Vojtek *et al*. (2019) investigated the sensitivity of the EBA4SUB hydrological parameters to flood mapping and found that the influence of the Curve Number on the hydrological model was more significant than that of the time of concentration. Annis *et al.* (2020) used EBA4SUB for effective flood mapping in Italy's ungauged Marta basin, using drone derived elevation data combined with the hydrograph obtained from EBA4SUB to map the extent of the flood. Petroselli *et al*. (2020) provided a full sensitivity analysis of the model, selecting four case studies in Italy. Finally, Petroselli (2020) upgraded the model, which was initially developed for considering only the surface flow, also introducing the subsurface flow.

This study employed the EBA4SUB model for determining the design peak flow in the watersheds of Kakia and Esamburumbur in Narok town, Kenya. As explained below, although the EBA4SUB model can work in the fully ungauged basin situation, by automatically calibrating its parameters for assessing the design hydrograph and, at the same time, minimising the user subjectivity, in this specific case, the model was first calibrated using observed flood data. Later the results of the modelling were compared with the results of rainfall frequency analysis in the sub-watersheds, previously performed by Houessou-Dossou *et al*. (2019). The aims of the present manuscript are hence: i) the first application of EBA4SUB rainfall-runoff model in Narok town, Kenya; and ii) the assessment of the relationship between design rainfall and design discharge, a circumstance that was never investigated in previous studies related to the model.

Materials and methods

Description of the EBA4SUB rainfall-runoff model

EBA4SUB (Grimaldi and Petroselli 2015; Piscopia *et al.* 2015) is an event-based rainfall-runoff model consisting of the following modules: i) gross rainfall estimation; ii) excess rainfall estimation; and iii) excess rainfall-direct runoff transformation.

i) Regarding the gross rainfall module, the user can employ an observed rainfall hyetograph recorded at the rain gauge; alternatively, IDF curves can be used, selecting the critical rainfall duration and the design hyetograph pattern. The Chicago hyetograph has been used here, consisting of two empirical equations (Eqs. 1 and 2), the first valid before the peak time and the second after the peak time. When using the Chicago method, the rainfall duration and peak position must be carefully selected, primarily because high peak time can lead to overestimating design flow (Mazurkiewicz & Skotnicki, 2018). This is all the most important in flood mapping, where overestimating the peak flow can result in overestimating flood height (Olsson, 2019).

$$i(t,T) = a(T)n(T)\left(\frac{tp-t}{rc}\right)^{n-1} \quad \text{for } t \le tp \tag{1}$$

$$i(t,T) = a(T)n(T)\left(\frac{t-tp}{1-rc}\right)^{n-1} \quad \text{for } t \ge tp \tag{2}$$

In Eqs. 1 and 2, i (t, T) is the rainfall intensity (mm/h), t the time (h), T the return period (y), a (mm/h), and n (-) the IDF coefficients, tp the peak time (h), rc (-) the ratio between the peak time and rainfall duration. Here, an IDF with two parameters was considered (Piscopia *et al*., 2015). Eqs. 1 and 2 are used for a specific return period T and a critical rainfall duration. The critical rainfall duration is defined by default in EBA4SUB as equal to the basin concentration time (Tc), which is estimated thanks to the Giandotti formula (1934), retrieving the necessary information from the basin's DEM. Nonetheless, the user can vary the rainfall duration if a different value is preferred or if observed rainfall-runoff data are available, from which it is possible to argue the basin response time to rainfall. Since the Giandotti formula was developed for basins characterised by a contributing area greater than 170 km^2 (that is greater than the contributing area of the investigated case studies, as shown in the following), here we used the Kirpich (1940) formula, expressed by:

$$T_c = \left[\frac{0.948L^3}{H}\right]^{0.385} \tag{3}$$

Where T_c is the time of concentration (h), L is the length of the longest waterway from the point in question to the basin divide (km), and H is the difference in elevation between the watershed outlet and the basin divide (m). Both were using observed rainfall events or IDF curves with the desired rainfall duration; an areal reduction factor (ARF) can be applied to transform the point rain gauge information into a spatially uniform rainfall assigned to the whole catchment, according to the Leclerc and Schaake (1972) formulation.

ii) In the excess rainfall estimation module, the curve number for Green-Ampt (CN4GA) (Grimaldi *et al*., 2013) procedure is applied, merging two approaches. The first approach uses the empiric curve number (CN) method (NRCS, 2008) to determine ponding time and cumulative excess rainfall volume starting from cumulative gross rainfall volume and adopting the following equation:

$$\begin{cases} Pn = \frac{(P-Ia)^2}{P-Ia+S} \\ S = \frac{1000}{CN} - 10 \end{cases} \quad (4)$$

Where Pn is the cumulate excess rainfall (mm); P is the cumulate gross rainfall (mm) as provided by IDF curves; S is the potential maximum retention of water by the soil (mm); Ia is the Initial quantity of interception, depression, and infiltration (mm). It is noteworthy that the NRCS CN method does not consider rainfall intensity and does not include the temporal infiltration process in the runoff modelling; therefore, the method is not suitable for sub-daily modelling (Walega *et al*., 2020). As a result, the Green and Ampt (GA) infiltration model (Green and Ampt, 1911) is used as a second approach to model the infiltration and excess rainfall within a specific event at the desired time resolution. The GA method is expressed by the following:

$$f(t) = K(\frac{\varphi\Delta\theta}{F(t)} + 1) \quad (5)$$

Where *f*(t) is the infiltration rate (mm/h); K is the hydraulic conductivity (mm/h); φ is the wetting front soil suction head (mm); Δθ represents the change in moisture content (-); F(t) is the cumulative infiltration (mm); t is the time (h). In EBA4SUB, the CN and GA approaches are mixed as follows. In the first step, the CN method is applied to determine ponding time and cumulative excess rainfall starting from cumulative gross rainfall. The second step distributes the cumulative excess rainfall volume in time, within the assumed event duration, and with the desired sub-event resolution, according to the GA equation, calibrating the equation parameters automatically. Finally, CN4GA is implemented assuming that the ponding time occurs when total gross rainfall equals Ia. The excess rainfall estimated using CN4GA has the same cumulative excess value and the same initial abstraction value derived with the CN method, but it has a physically-based time distribution, thanks to the application of the GA method. The only needed parameter for applying the CN4GA procedure is CN, since the GA parameters are estimated automatically. CN can be estimated by default in EBA4SUB using look-up tables linking its value to land use and soil data, or it can be specified by the user if observed rainfall-runoff data are available, from which it is possible to argue the relationship between gross rainfall, excess rainfall, and cumulative infiltration values.

iii) In the excess rainfall-direct runoff transformation, the design hydrograph Q(t) is determined using the basin's hydrological characteristics and by employing a parsimonious geomorphological instantaneous unit hydrograph (IUH) which is based on the width function framework (WFIUH) (Grimaldi *et al.,* 2012), thanks to the convolution integral expressed by:

$$Q(t) = A\int_0^t WFIUH(t-\tau)P_n(\tau)d\tau \quad (6)$$

Where A is the area of the watershed (m^2), t is the time (s), and $P_n(t)$ (m/s) is the excess rainfall calculated using the CN4GA approach. For example, in the previous equation, the WFIUH is expressed as follows:

$$WFIUH(t) = \frac{L_c(x)}{v_c(x)} + \frac{L_h(x)}{v_h(x)} \quad (7)$$

Where L_h (m) is the hillslope path, L_c (m) is the channel path of the DEM cell x, v_h (m/s) is the hillslope velocity, and v_h (m/s) is the channel flow velocity. The hillslope flow velocities are defined for each pixel employing a formula linking velocity to local slope and land cover. In contrast, for the channel pixels, the river velocity is calibrated, imposing that the projection of the WFIUH mass centre on the time axis is equal to the basin lag time (T_L), which is estimated as 60% of the concentration time, previously determined. From a methodological point of view, EBA4SUB is characterised by two main advantages. First, in excess rainfall estimation, it combines the simplicity of an empirical approach (the CN method) with the accuracy of a physically-based infiltration scheme (the GA equation). Second, for excess rainfall-direct runoff transformation, the IUH shape is determined using detailed geomorphological information on every basin pixel, and the use of synthetic shapes is avoided.

Study areas and data

This study was conducted in the ungauged basin formed by Kakia and Esamburumbur sub-watersheds in Narok town, Kenya (Figure 1). The total contributing areas are 30.6 km^2 for Kakia and 15.6 km^2 for Esamburumbur. Kakia and Esamburumbur are two ephemeral streams that, during the rainy season, turn into rivers, causing flooding in Narok town, located at the confluence of the two rivers, a phenomenon that is under study under the current project '*Flash flood and Erosion in Enkare Narok Basin, Kenya: causes and management*.' A TAHMO (Trans-African Hydro-Meteorological Observatory) automatic weather station is located upstream in the Kakia watershed at Latitude 1.012996° S, Longitude 35.899120° E, and an elevation of 2122 m (see Figure 1), and rainfall intensity measurements are available from 7 December 2018 at 15 minute time intervals.

In the lower sections within the town, the Esamburumbur and Kakia channels have been lined with concrete, and a water level gauge was marked at outlets O1 and O2 (see Figure 2), respectively, and discharge was measured for two flood events: the events of 01 September 2019 and 28 December 2019. Table 1 summarises the observed discharge in Kakia and Esamburumbur. To compare

Table 1. Observation in Kakia and Esamburumbur.

Date	Total precipitation at TAHMO station (mm)	Rainfall duration (h)	Observed Qpeak (m^3/s) at outlet O1 in Esamburumbur	Observed Qpeak (m^3/s) at outlet O2 in Kakia
1-Sep-19	22.4	3.75	None	44.26
28-Dec-19	17.6	2.50	45.90	8.34

the rainfall frequency analysis (Houessou-Dossou *et al*., 2019) with the flood frequency analysis in Narok town, the design hydrographs have been calculated using EBA4SUB for 1, 5, 10, 25, 50, and 100 years return period at O1 and O2. O1 represents the outlet of Sub-watershed W1 (in Esamburumbur), and O2 represents the outlet of sub-watershed W2 (in Kakia) (Figure 2).

The used data were acquired from different sources and pertain to DEM with 30 m resolution, soil hydrological group, land use/land cover map of W1 and W2, and the IDF curve of Narok. The DEM was used by EBA4SUB to extract the river network and compute the WFIUH. The 30 m resolution SRTM DEM of the sub-watersheds was downloaded from http://geoportal.rcmrd.org/. The DEM was used to process the flow direction and accumulation grids for the two watersheds. The elevation within sub-watershed W1 varies from 1848 to 2097 m, while the elevation within W2 varies from 1859 to 2138 m. The average slope in W1 (6.78%) is higher than in W2 (5.48%).

Regarding land use, many studies have demonstrated the influence of land use/land cover on the surface runoff (*e.g*., Yin *et al*., 2017). The land use/land cover map of W1 and W2 were extracted from the Kenyan land use/land cover map with a 30 m resolution, established in 2015which is available on ICPAC (Igad Climate Prediction & Applications Centre) website at http://geoportal.icpac.net/layers/geonode%3Akenyalandcover2015. The two sub-watersheds are dominated by agricultural land use, covering 76.9% of W1 and 89.5% of W2. EBA4SUB uses 'CORINE (Coordination of Information on the Environment)' land cover nomenclature at level III (Bossard *et al*., 2000) to assign the hillslope flow veloci-

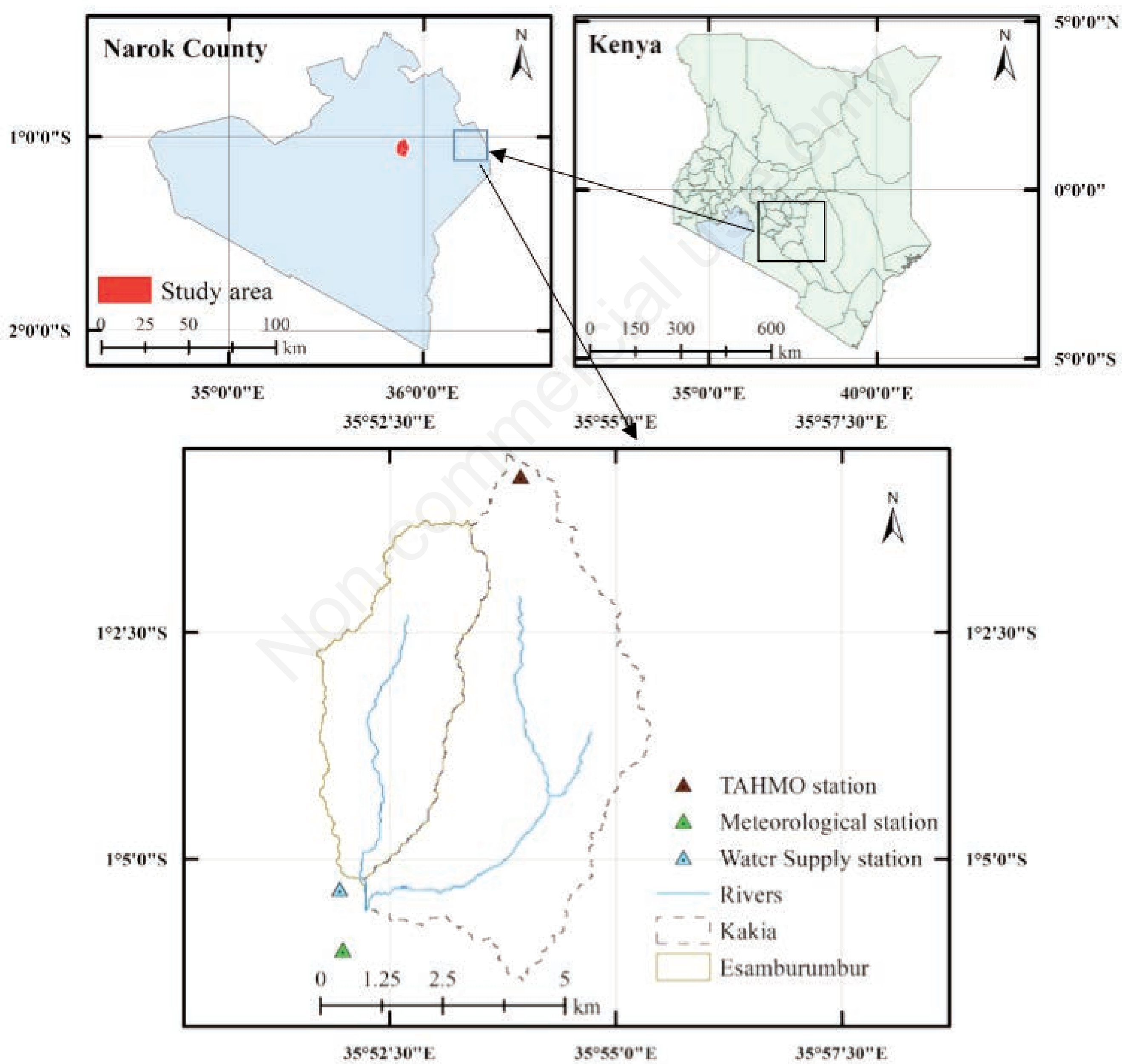

Figure 1. Location of the study area in Narok, Kenya.

ties and compute the CN values. Therefore, the land use/land cover was classified accordingly. Moreover, the watersheds' hydrological soil group was extracted from the global hydrological soil group accessible at https://daac.ornl.gov/SOILS/guides/Global_Hydrologic_Soil_Group.html. The dataset represents a globally consistent soil group at 250 m resolution developed by the Food and Agriculture Organization (FAO) based on soil texture classes and depth (Ross *et al.,* 2018). W1 and W2 are dominated by soil group C, the texture of which is clay loam.

Figure 3 presents the DEM, drainage network, and land use/land cover in W1, while Figure 4 presents the DEM, drainage network, and land use/land cover in W2. In both figures, the land use/land cover corresponding to the Corine Nomenclature is as follows: 111-Continuous urban fabric; 211-Non-irrigated arable agricultural land; 313-Mixed forest; 321-Natural grasslands; 324-Transitional woodland-shrub; 333-Sparsely vegetated areas; 411-Inland marshes.

The IDF curves were extracted for Narok town as published in the Rainfall Frequency Atlas of Kenya (Kenya Ministry of Water Development, 1978) and reported in Table 2 and shown in Figure 5. Narok IDF allows us to obtain the rainfall intensity corresponding to a specific duration for a given return period. Narok IDF curves were used to estimate the gross rainfall depth for 1, 5, 10, 25, 50, and 100 years return period. The Chicago hyetograph was adopted to convert the gross rainfall to a hyetograph. A peak position equal to 0.5 was selected, and the ARF was used. We selected the Chicago hyetograph because it usually favours safety since it produces higher values of peak discharge (Petroselli *et al*., 2020). Moreover, we assumed a peak position equal to 0.5 due to the contribution of Piscopia *et al*. (2015), who found that the peak position

Table 2. Narok intensity-duration-frequency parameters for 1, 5, 6, 10, 25, 50, and 100 years return period.

IDF parameters	Return period					
	1	5	10	25	50	100
a	32.33	44.11	51.57	60.98	67.76	76.36
n	0.59	0.59	0.60	0.60	0.60	0.60

IDF, intensity-duration-frequency.

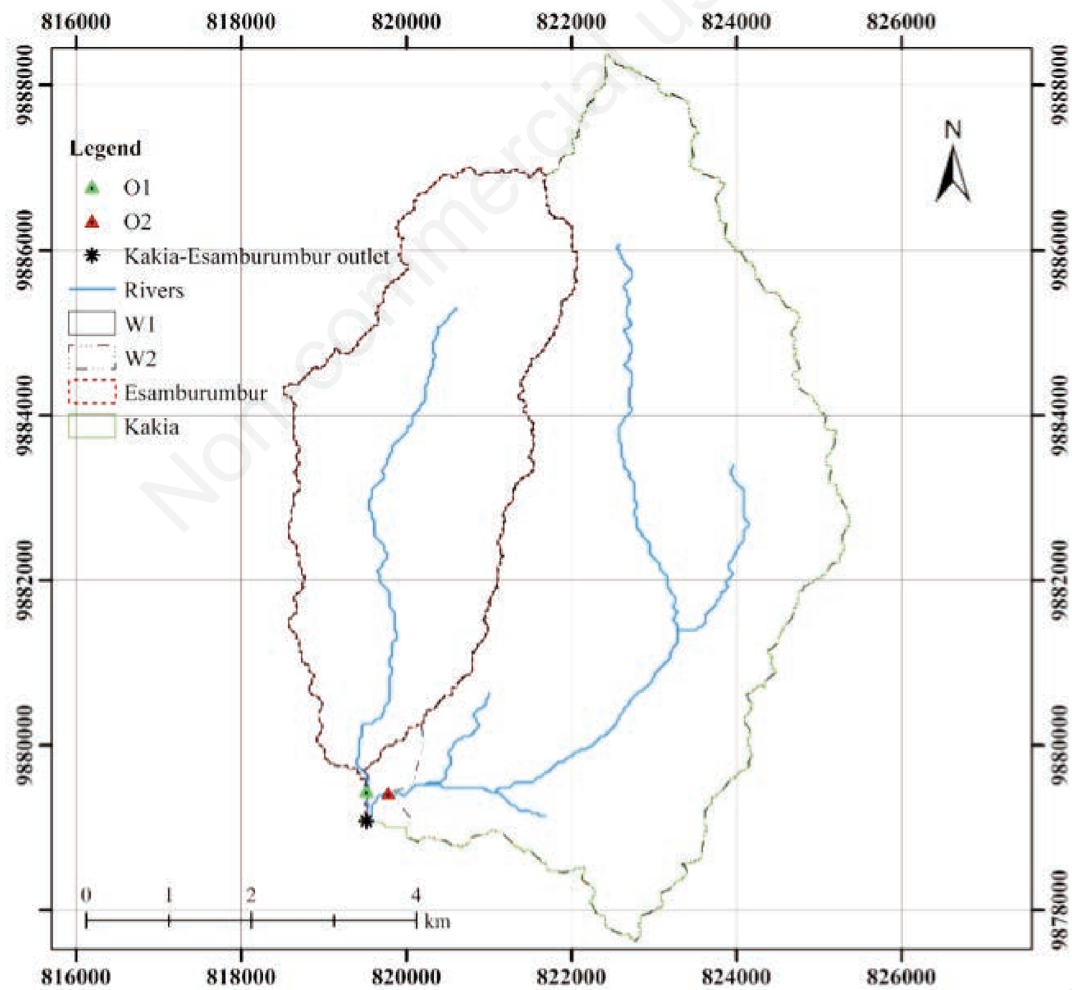

Figure 2. Location of O1, O2, W1, and W2 in Esamburmbur (left side) and Kakia (right side) sub-watersheds in Narok town, Kenya.

does not sensibly affect peak flow, recommending the use of 0.5.

As previously described, the excess rainfall estimation is estimated using the design hyetograph and CN4GA approach. In the present study, the CN value was calibrated in order to reach, for the observed rainfall-runoff events, a value of modelled peak discharge equal to the observed value. It is noteworthy that only the peak discharge value is available for the observed events, not the whole hydrograph. Such circumstance does not allow to infer the basin response time to rainfall, so calibration of Tc is questionable. Hence, for Tc, we decided to use the values provided by the Kirpich formula, as previously specified.

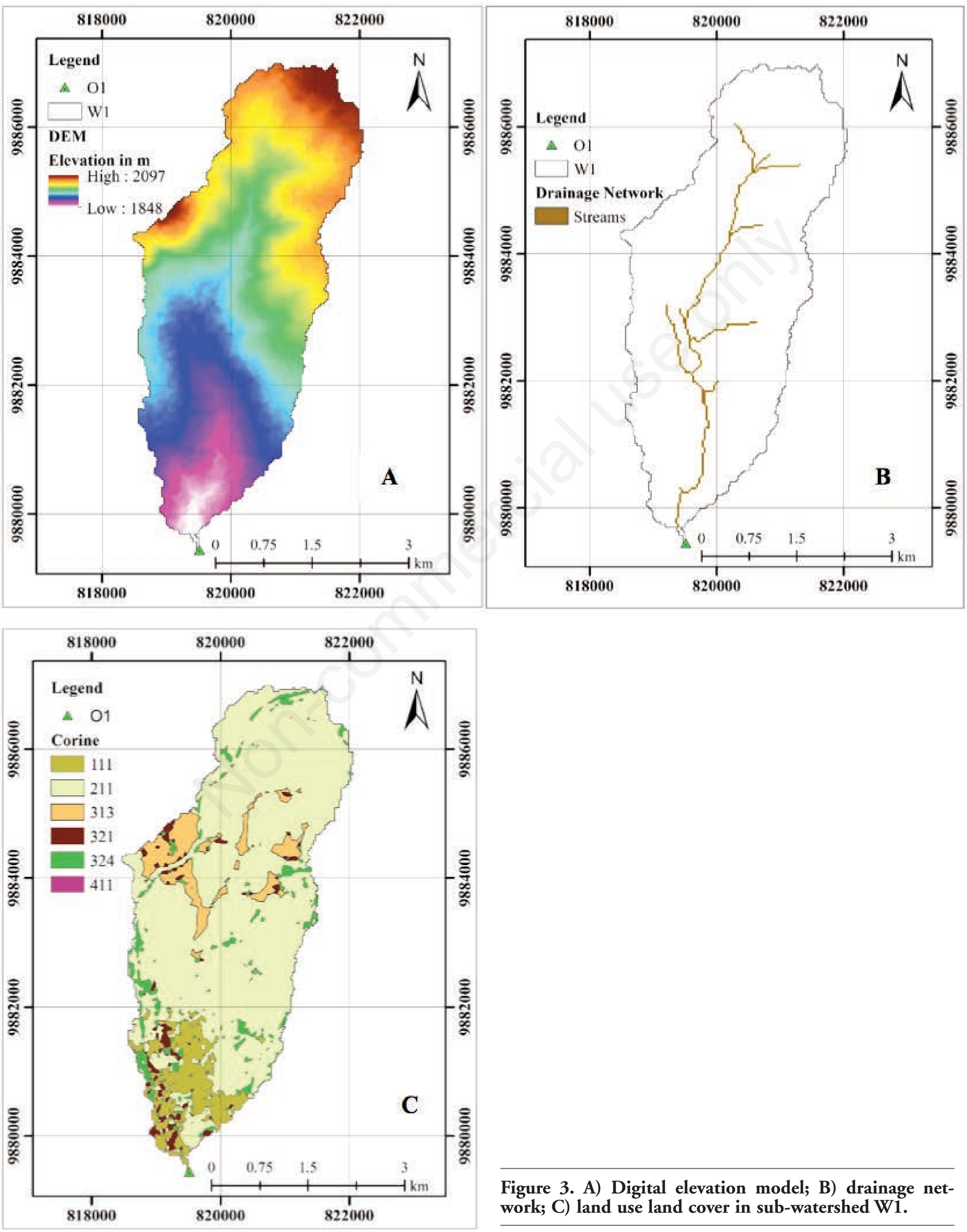

Figure 3. A) Digital elevation model; B) drainage network; C) land use land cover in sub-watershed W1.

Results and discussion

Regarding the design hydrograph estimation, WFIUH has been estimated for both sub-watersheds using the DEM and the concentration time, estimated using the Kirpich formula. A 15-minute time resolution was chosen for the WFIUH to accurately represent the topographic information (Petroselli & Grimaldi, 2018). The DEMs were pre-processed to remove the spurious points like pits and flat areas using SAGA GIS (System for Automated Geoscientific Analyses). Table 3 presents the sub-watersheds characteristics, while the WFIUH for W1 (Esamburumbur) and W2 (Kakia) are displayed in Figure 6.

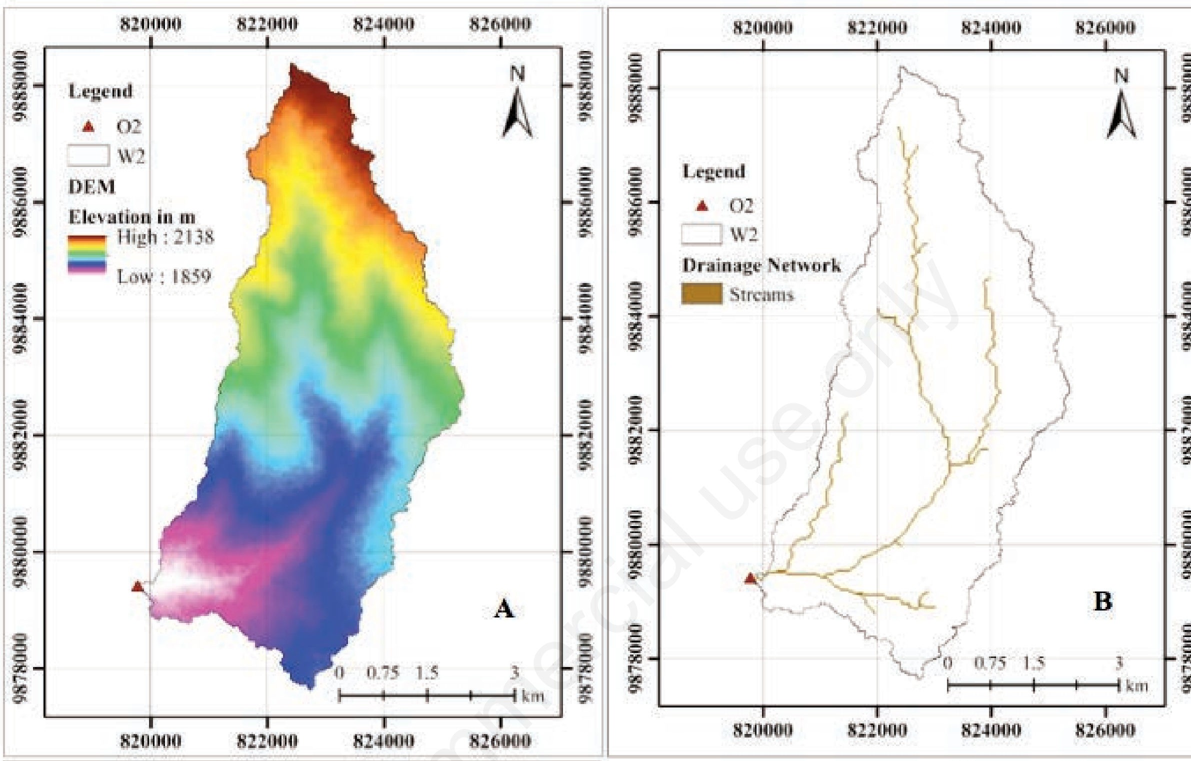

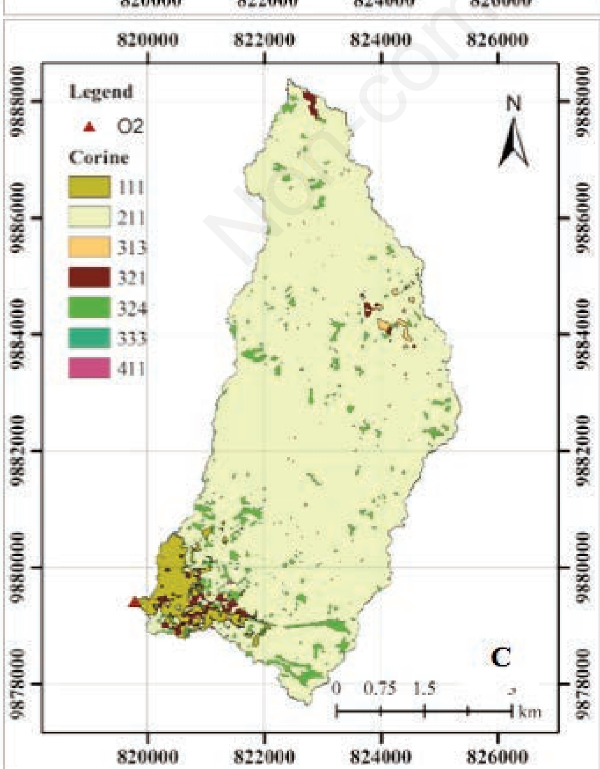

Figure 4. A) Digital elevation model; B) drainage network; C) land use land/cover-up in sub-watershed W2.

As shown in Figure 6, the watershed topography highly affects the shape of the WFIUH (Bajracharya and Jain, 2020). The shape of the WFIUH varies in both sub-watersheds. The WFIUH exhibits smooth behaviour in W2 while showing a rough shape in W1. The WFIUH shows an increasing trend in the contributing area with time in W1, followed by a decreasing trend where a peak (0.24) was reached at 45 minutes. In W2, the peak (0.17) was reached at 60 minutes. Moreover, the sub-watershed W1 displayed a higher value for the WFIUH peak. The reason for this is that the slope of W1 is higher (6.78%) than that of W2 (5.48%). The basin slope controls the flow velocity in the watershed, and therefore it affects the WFIUH shape (He, 2007).

Comparison of observed and simulated peak flow in W1 and W2

The calculated value of Tc is respectively 1.15 hours in W1 and 1.8 hours in W2. Compared with observation, EBA4SUB has performed well in W1 and W2 for the two events considered (Table 4). The absolute difference obtained was 0.3 m^3/s in W1 in Esamburumbur and 0.12 m^3/s in W2 in Kakia. In addition, the corresponding CN values were 96.6 in W1 for the event of 28 December 2019 and 85.1 in W2 for the same event. Nevertheless, a lower CN value was noted for the case of 1 September 2019 (CN=93.5). The calculation of CN is primarily based on the AMC, which differs from a rainfall event. As a result, drier soil often results in a lower CN value and thus a small runoff than wetter soil (Gundalia and Dholakia, 2014). Moreover, according to Ponce and Hawkins (1996), the characteristics of watersheds and land use, the intensity of the storm, and the quality of the observation may also explain the variability of the CN for different events. Since we have no other information, we decided to adopt, for the Kakia basin, a calibrated value for CN that is the average value of the two observed CNs.

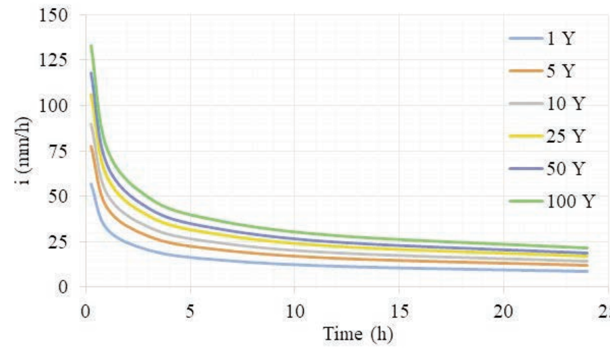

Figure 5. Intensity-duration-frequency curves of Narok town for the different return periods. ***Source: Kenya Ministry of Water Development, 1978.***

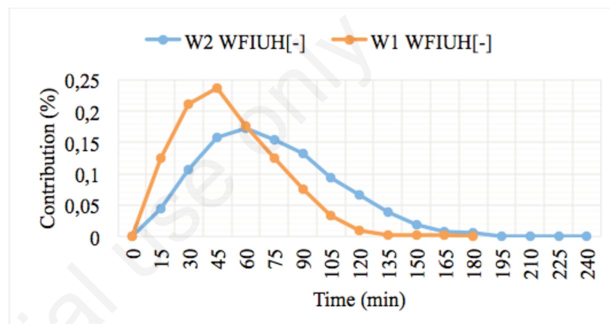

Figure 6. Width function instantaneous unit hydrograph (WFIUH) in W1 and W2.

Table 3. Sub-watersheds W1 and W2 characteristics.

Characteristics	W1 in Esamburumbur	W2 in Kakia
Area (km^2)	15.6 (from inlet to O1)	30.1 (from inlet to O2)
Maximum sub-basin elevation (m)	2097	2138
Outlet elevation (m)	1848	1859
Length of the main channel (km)	7.25	11.09
Tc (h)	1.15	1.8

Table 4. Observed and simulated peak flow at outlets O1 in Esamburumbur and O2 in Kakia.

W1 in Esamburumbur				
Date	Measured Qp (m^3/s)	Tc (h)	CN	Qp-EBA4SUB (m^3/s)
1-Sep-19		-	-	-
28-Dec-19	45.90	1.15	96.6	45.6
	Calibrated values	1.15	96.6	
W2 in Kakia				
Date	Measured Qp (m^3/s)	Tc (h)	CN	Qp-EBA4SUB (m^3/s)
1-Sep-19	44.26	1.8	93.5	44.2
28-Dec-19	8.34	1.8	85.1	8.4
	Calibrated values	1.8	89.3	

Design hydrograph analysis in W1 and W2 for 1, 5, 10, 25, 50, and 100 years return period

Regarding the design hydrograph calculation, Figures 7 and 8 show the gross rainfall hyetograph, rainfall excess hyetograph, and design hydrograph in W1 and W2, respectively, for 1, 5, 10, 25, 50, and 100 years. In both sub-watersheds, the position of the peak rainfall excess is preserved for the different return periods. This confirms the findings of Petroselli and Grimaldi (2018), where it was shown that the CN4GA method can preserve the peak position of the excess rainfall within the gross rainfall. However, for a particular return period, the excess and gross rainfall are lower in W1

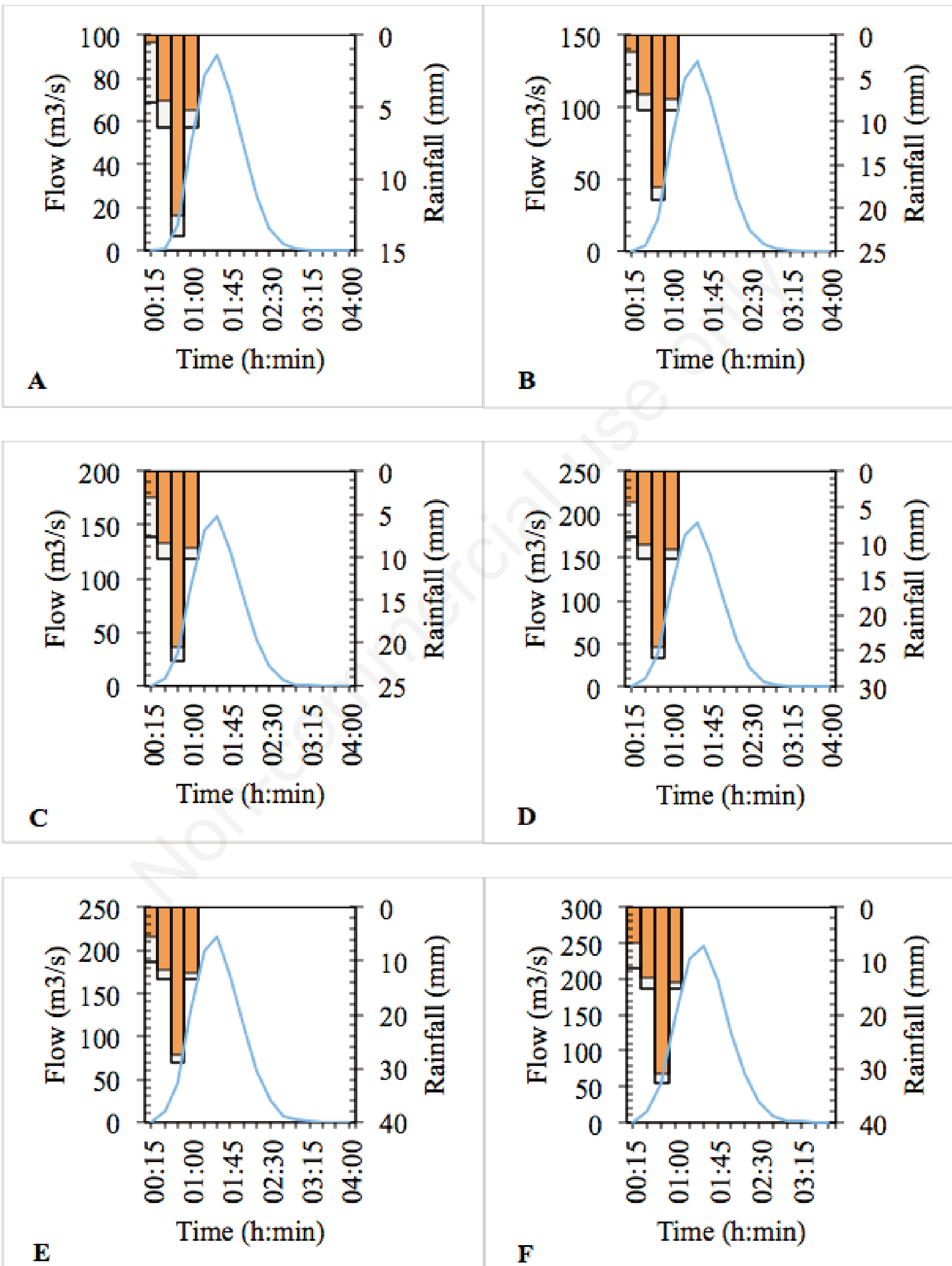

Figure 7. Gross hyetograph (in light grey), excess rainfall hyetograph (in orange), and design hydrograph (in blue) in W1 in Esamburumbur for: A) 1 year; B) 5 years; C) 10 years; D) 25 years; E) 50 years; and F) 100 years return period.

than W2, mainly because W1 is smaller in size and characterized by a short time of concentration that determines the rainfall duration. Also, the cumulative gross rainfall increases with the return period, ranging from 31.5 mm for 1 year of the return period to 74.3 mm for 100 years in W1 (Table 5) and from 43.6 mm for 1 year of the return period to 103.6 mm for 100 years in W2. Figures 7 and 8 also show that the rainfall duration is longer in W2 than W1 since W2 is more significant in size (Abdullah, 2013), consequently, the peak flow is reached sooner in W1. Also, it was noticed that after the beginning of runoff, the runoff takes less time

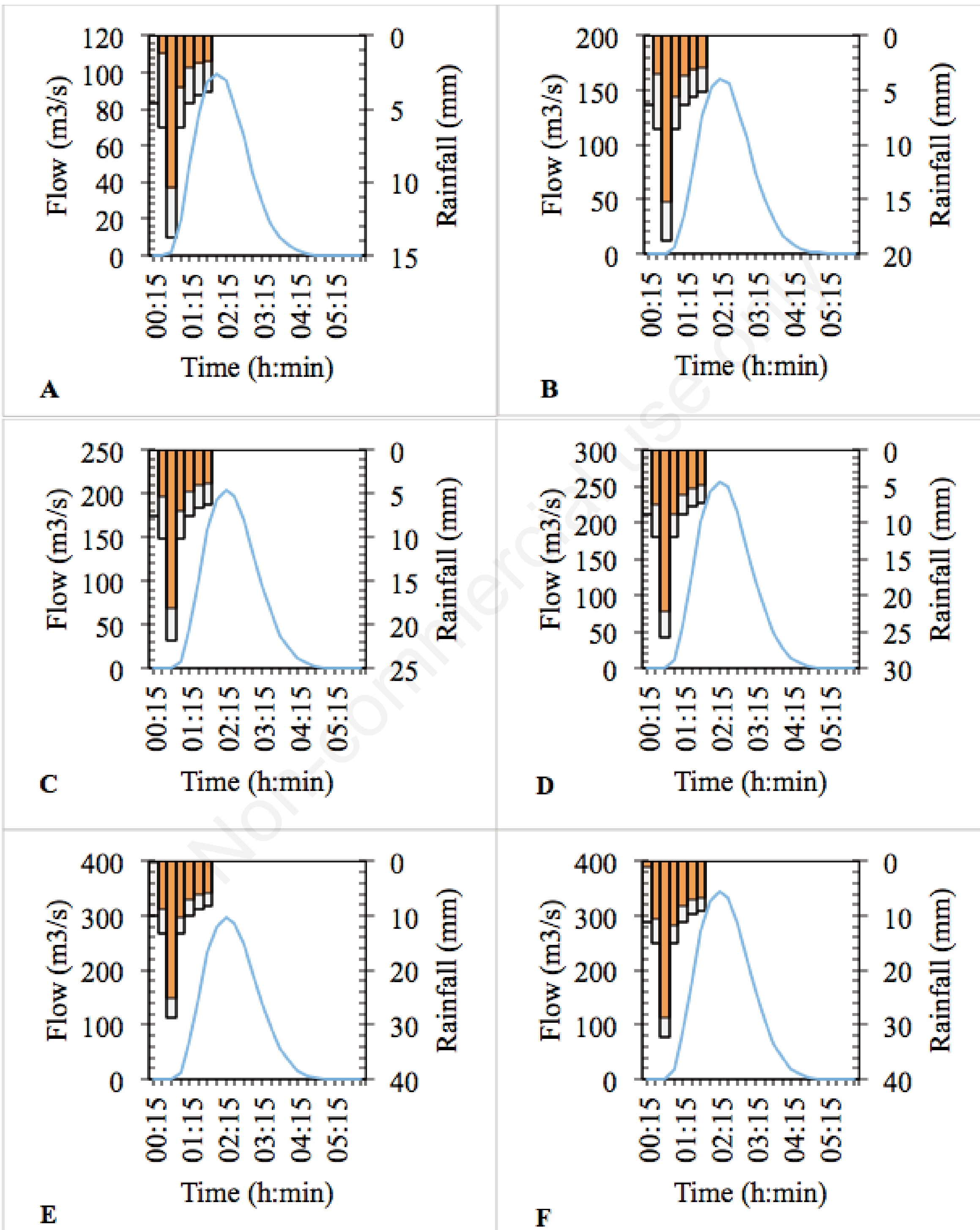

Figure 8. Gross hyetograph (in light grey), excess rainfall hyetograph (in orange), and design hydrograph (in blue) in W2 in Kakia for (A) 1 year; (B) 5 years; (C) 10 years; (D) 25 years; (E) 50 years and (F) 100 years return period.

(1.5 hours in W1 and 2 hours in W2) to reach its peak. This often characterises small streams where runoff enters the river very quickly (Gleick, 1996). The hydrograph time base is also greater in W2 than W1, which is the direct consequence of the time of concentration in W2. The slope of the channel could also influence this. For example, for a larger slope, a smaller time base of the hydrograph is caused by the quick rise of the depletion of storage followed by a steeper recession limb (He, 2008).

Table 5 reports the cumulative values for gross rainfall, excess rainfall, flow volume, plus the value of peak flow in W1 and W2 for 1, 5, 10, 25, 50, and 100 years return period. The watershed W1 is the smallest sub-watershed and has recorded lower peak flow and, therefore, lower volume. For instance, the total volume in W1 was 356,904 m^3 compared to a total volume in W2 of 623,118 m^3 for T=1 year. Moreover, the higher volume within W2 for the different events may be attributed to the loss of vegetation cover in the sub-watershed due to the inadequate cultivation practices, which often result in the decrease of the soil infiltration rate and the increase of runoff volume. A more detailed study may be needed to evaluate the impact of land-use change on the flow volume in the sub-watersheds.

A final consideration concerns the quality and resolution of EBA4SUB input parameters, potentially affecting the modelled results. As shown in Petroselli *et al.* (2020), CN and Tc can be regarded as primary parameters, so they should be estimated with particular attention, while rainfall and WFIUH temporal resolution, DEM spatial resolution, and design hyetograph shape can be considered secondary parameters, not particularly influencing the hydrograph shape.

Comparison of flood and rainfall frequency analysis

The results of flood frequency analysis were compared with the results of rainfall frequency analysis (Houessou-Dossou *et al.,* 2019). Figures 9 and 10 illustrate the correlation between the rainfall-based return period and the flood-based return period in Esamburumbur and Kakia, respectively. The statistics show a high correlation between the rainfall frequency analysis and the flood frequency analysis for the different return periods, with a coefficient of determination of 0.99 in the sub-watersheds of both Kakia and Esamburumbur. The correlation obtained between the flood frequency analysis and the rainfall frequency analysis for the 1, 5, 10, 25, 50, and 100-year events showed a parabolic relationship in the studied sub-watersheds between the rainfall return period and the flow-based return period. According to the CN approach, this could be attributed to the non-linear transformation of gross rainfall in excess rainfall. Indeed, it is true that Viglione and Bloschl (2008) established that the rainfall-based return period and flow-based return period in the case of a single storm duration, a con-

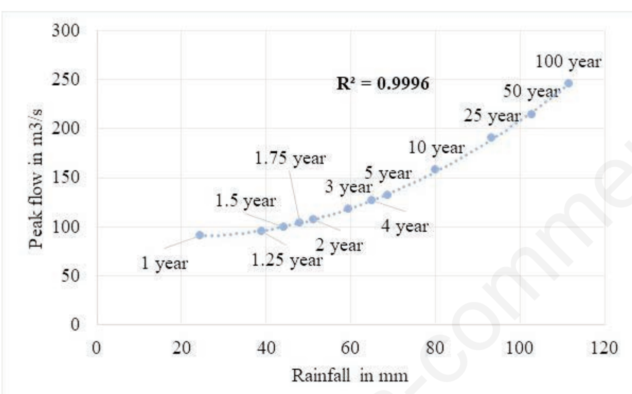

Figure 9. Correlation between flood frequency analysis and rainfall frequency analysis in W1 in Esamburumbur.

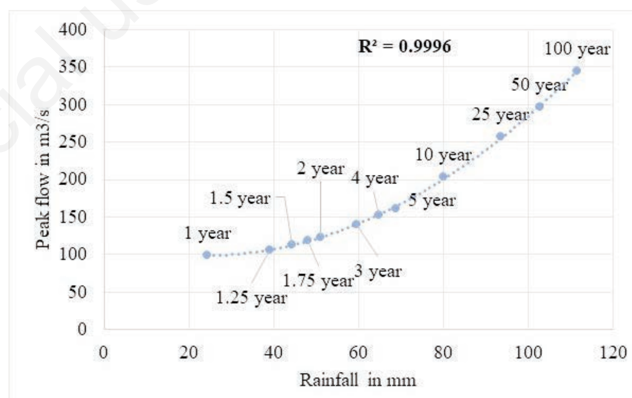

Figure 10. Correlation between flood frequency analysis and rainfall frequency analysis in W2 in Kakia.

Table 5. Total gross rainfall, rainfall excess, volume, and peak flow in W1 and W2 for the different return periods.

Return period (year)	Watershed	Total gross rainfall (mm)	Total rainfall excess (mm)	Peak flow (m^3/s)	Volume (m^3)
1	W1	31.5	22.8	90.9	356,904
	W2	43.6	20.7	99.1	623,118
5	W1	42.9	33.8	131.9	528,887
	W2	59.5	34.0	161.0	1,023,380
10	W1	50.2	40.9	157.7	639,379
	W2	69.9	43.2	203.3	1,300,974
25	W1	59.4	49.9	191.0	779,686
	W2	82.7	54.8	257.0	1,649,703
50	W1	66.0	56.3	215.0	881,244
	W2	91.9	63.3	296.3	1,905,761
100	W1	74.4	64.6	245.6	1,010,460
	W2	103.6	74.3	345.3	2,234,815

stant runoff coefficient, and a linear basin response are the same, but EBA4SUB does not use the runoff coefficient; instead, it uses the CN scheme.

Moreover, in the research by Dickinson *et al*. (1992), a strong relationship in the examined small watersheds between extreme flows induced by extreme rainfall was noted. However, the authors pointed out that extreme rainfall does not always produce an extreme flow. Zhu *et al*. (2017) observed a larger return period for peak discharge quantiles in wet antecedent soil moisture conditions than the rainfall that produced them, with a reverse in dry conditions.

Conclusions

This study evaluated the EBA4SUB rainfall-runoff model for design peak flow estimation in the ungauged sub-watersheds of Kakia and Esamburumbur in Narok, Kenya. The novelty of the study was the first application of the recently developed EBA4SUB model in Kenya. Moreover, in this study, the peak flow-based return period was compared to the rainfall-based return periods, and this is the first time unlike previous studies where EBA4SUB was employed. The results have shown a strong link between modelled flood frequency analysis and modelled rainfall frequency analysis. Moreover, the relationship between modelled flood frequency analysis and modelled rainfall frequency analysis showed a parabolic behaviour. The study showed the relevance of the proposed method for estimating design hydrograph in ungauged basins while showing the link between rainfall frequency analysis and flood frequency analysis in small watersheds. The output of the study can be relevant for flood risk management and hydraulic design.

References

Abdullah J. 2013. Distributed runoff simulation of extreme monsoon rainstorms In Malaysia using TREX. Doctoral Dissertation, Colorado State University.

Ahmed M., Sultan M., Elbayoumi T., Tissot P. 2019. Forecasting GRACE data over the African watersheds using artificial neural networks. Remote Sens. 11:1769.

Annis A., Nardi F., Petroselli A., Apollonio C., Arcangeletti E., Tauro F., Belli C., Bianconi R., Grimaldi S. 2020. UAV-DEMs for small-scale flood hazard mapping. Water 12:1717.

Beck H.E., van Dijk A.I., De Roo A., Miralles D.G., McVicar T.R., Schellekens J., Bruijnzeel L.A. 2016. Global□scale regionalization of hydrologic model parameters. Water Resour. Res. 52:3599-622.

Bossard M., Feranec J., Otahel J. 2000. CORINE land cover technical guide: Addendum 2000. Available from: https://www.researchgate.net/profile/Jan_Otahel/publication/268745953_Corine_Land_Cover-Technical_Guide/links/5b4f3e9daca27217ff9f8489/Corine-Land-Cover-Technical-Guide.pdf

Dhakal N., Fang X., Cleveland T.G., Thompson D.B., Asquith W.H., Marzen L.J. 2012. Estimation of volumetric runoff coefficients for Texas watersheds using land-use and rainfall-runoff data. J. Irrig. Drain. Eng. 138:43-54.

Dickinson W.T., Whiteley H.R., Kelly P.N. 1992. Extremes for rainfall and streamflow, how strong are the links?. Can. Water Resour. J. 17:224-36.

Giandotti M. 1934. Previsione delle piene e delle magre dei corsi d'acqua (Estimation of floods and droughts of rivers). Istituto Poligrafico Dello Stato 8:107-17.

Gleick P.H. 1996. Water resources. In: Schneider S.H. (Ed.), Encyclopedia of climate and weather. Oxford University Press, New York, 2:817-23.

Green W.H., Ampt G.A. 1911. Studies on soil physics. J. Agric. Sci. 4:1-24.

Grimaldi S., Petroselli A., Nardi F. 2012. A parsimonious geomorphological unit hydrograph for rainfall-runoff modelling in small ungauged basins. Hydrolg. Sci. J. 57:73-83.

Grimaldi S., Petroselli A., Romano N. 2013. Curve-Number/Green-Ampt mixed procedure for streamflow predictions in ungauged basins: parameter sensitivity analysis. Hydrol. Process. 27:1265-75.

Grimaldi S., Petroselli A. 2015. Do we still need the rational formula? An alternative empirical procedure for peak discharge estimation in small and ungauged basins. Hydrol. Sci. J. 60:67-77.

Gundalia M., Dholakia M. 2014. Impact of monthly curve number on daily runoff estimation for Ozat catchment in India. Open J. Modern Hydrol. 4:144.

He X. 2008. Unit hydrograph estimation using digital drainage model for applicable Texas Watersheds. Doctoral Dissertation, University of Houston.

Houessou-Dossou E.A.Y., Mwangi Gathenya J., Njuguna M., Abiero Gariy Z. 2019. Flood frequency analysis using participatory GIS and rainfall data for two stations in Narok Town, Kenya. Hydrology 6:90.

Jian J., Ryu D., Costelloe J.F., Su C.H. 2017. Towards hydrological model calibration using river level measurements. J. Hydrol. Reg. Stud. 10:95-109.

Leclerc G., Schaake J.C. 1972. Derivation of hydrologic frequency curves. Report 142, Mass. Inst. of Technol., Cambridge, 151.

Ministry of Water Development. 1978. Rainfall frequency atlas of Kenya. Ministry of Water Development, Nairobi, Kenya.

Kirpich Z.P. 1940. Time of concentration of small agricultural watersheds. Civil Eng. 10:362.

Mazurkiewicz K., Skotnicki M. 2018. A determination of the synthetic hyetograph parameters for flow capacity assessment concerning stormwater systems. In E3S Web of Conferences. 45:00053.

Młyński D, Petroselli A, Wałęga A. 2018. Flood frequency analysis by an event-based rainfall-Runoff model in selected catchments of southern Poland. Soil Water Res. 13:170-6.

Młyński D., Wałęga A., Książek L., Florek J., Petroselli A. 2020a. Possibility of using selected rainfall-runoff models for determining the design hydrograph in mountainous catchments: a case study in Poland. Water. 12:1450.

Młyński D., Wałęga A., Ozga-Zielinski B., Ciupak M., Petroselli A. 2020b. New approach for determining the quantiles of maximum annual flows in uncontrolled catchments using the EBA4SUB model. J. Hydrol. 589:125198.

NRCS (Natural Resources Conservation Service), 2008. National engineering handbook - part 630, Hydrology. U.S. Department of Agriculture, Washington, DC, USA.

Olsson J. 2019. The influence of storm movement and temporal variability of rainfall on urban pluvial flooding: 1D-2D modelling with empirical hyetographs and CDS-rain. Master's thesis Uppsala University.

Pagliero L., Bouraoui F., Diels J., Willems P., McIntyre N. 2019. Investigating regionalization techniques for large-scale hydrological modelling. J. Hydrol. 570:220-35.

Petroselli A., Grimaldi S. 2018. Design hydrograph estimation in

small and fully ungauged basins: a preliminary assessment of the EBA4SUB framework. J. Flood Risk Manag. 11:S197-210.
Petroselli A., Vojtek M., Vojteková J. 2019a. Flood mapping in small ungauged basins: a comparison of different approaches for two case studies in Slovakia. Hydrology Res. 50:379-92.
Petroselli A., Mulaomerović-Šeta A., Lozančić Ž. 2019b. A comparison of methodologies for design peak discharge estimation in selected catchments of Bosnia and Herzegovina. Gradevinar 71:729-39.
Petroselli A., Asgharinia S., Sabzevari T., Saghafian B. 2019c. Comparison of design hydrograph estimation methods for ungauged basins in Iran. Hydrol. Sci. J. 65:127-37.
Petroselli A., Piscopia R., Grimaldi S. 2020. Design discharge estimation in small and ungauged basins: EBA4SUB framework sensitivity analysis. J. Agric. Eng. 51:107-18.
Petroselli A. 2020. A generalization of the EBA4SUB rainfall-runoff model considering surface and subsurface flow. Hydrol. Sci. J. 65:2390-401.
Piscopia R., Petroselli A., Grimaldi S. 2015. A software package for predicting design-flood hydrographs in small and ungauged basins. J. Agric. Eng. 46:74-84.
Ponce V.M., Hawkins R.H. 1996. Runoff curve number: Has it reached maturity?. J. Hydrol. Eng. 1:11-9.
Recanatesi F., Petroselli A., Ripa M.N., Leone A. 2017. Assessment of stormwater runoff management practices and BMPs under soil sealing: a study case in a peri-urban watershed of the metropolitan area of Rome (Italy). J. Environ. Manag. 201:6-18.
Recanatesi F., Petroselli A. 2020. Land Cover Change and flood risk in a peri-urban environment of the Metropolitan area of Rome (Italy). Water Resour. Manag. 34:4399-413.
Ross C.W., Prihodko L., Anchang J., Kumar S., Ji W., Hanan, N. P. 2018. Global hydrologic soil groups (HYSOGs250m) for curve number-based runoff modeling. ORNL DAAC, Oak Ridge, Tennessee, USA. Available from: https://daac.ornl.gov/cgibin/download.pl?ds_id=1566&source=schema_org_metadata
Song J., Xia J., Zhang L., Wang Z., Wan H., She D. 2016. Streamflow prediction in ungauged basins by regressive regionalization: A case study in Huai River Basin, China. Nord. Hydrol. 47:1053-68.
Viglione A., Blöschl G. 2009. On the role of storm duration in the mapping of rainfall to flood return periods. Hydrol. Earth Syst. Sci. 13:205-16.
Virães M.V., Cirilo J.A. 2019. Regionalization of hydrological model parameters for the semi-arid region of the northeast Brazil. RBRH 24.
Vojtek M., Petroselli A., Vojteková J., Asgharinia S. 2019. Flood inundation mapping in small and ungauged basins: sensitivity analysis using the EBA4SUB and HEC-RAS modeling approach. Hydrol. Res. 50:1002-19.
Walega A., Amatya D.M., Caldwell P., Marion D., Panda S. 2020. Assessment of storm direct runoff and peak flow rates using improved SCS-CN models for selected forested watersheds in the Southeastern United States. J. Hydrol. Reg. Stud. 27:100645.
Yang X., Magnusson J., Rizzi J., Xu C.Y. 2018. Runoff prediction in ungauged watersheds in Norway: comparison of regionalization approaches. Hydrol. Res. 49:487-505.
Yin J., He F., Xiong Y.J., Qiu, G.Y. 2017. Effects of land use/land cover and climate changes on surface runoff in a semi-humid and semi-arid transition zone in northwest China. Hydrol. Earth Syst. Sci. 21:183-96.
Zhu Z., Wright D.B., Yu G. 2018. The impact of rainfall space-time structure in flood frequency analysis. Water Resour. Res. 54:8983-98.